ACS Catalysis

pubs.acs.org/acscatalysis

Research Article

Identifying and Evading Olefin Isomerization Catalyst Deactivation Pathways Resulting from Ion-Tunable Hemilability

Henry M. Dodge, Matthew R. Kita, Chun-Hsing Chen, and Alexander J. M. Miller*

Cite This: *ACS Catal.* 2020, 10, 13019–13030

Read Online

ACCESS | Metrics & More | Article Recommendations | Supporting Information

ABSTRACT: Hemilabile ligands are found in many leading organometallic catalysts, but it can be challenging to tune the degree of hemilability in a particular catalyst. This work explores the impact of cation-tunable hemilability on the speciation of iridium(III) pincer-crown ether catalysts during high-activity olefin isomerization. Under conditions where strong cation−macrocycle interactions are fostered and terminal olefin has been consumed, labilization of the aza-crown ether group leads to an η^6-arene complex, wherein the pincer ligand is metallated at a different position. Arene complexes of styrene, naphthalene, and mesitylene were independently synthesized and found to exhibit diminished catalytic activity for allylbenzene isomerization. In response to these findings, a previously unreported catalyst bearing a synthetically modified pincer ligand was designed, resulting in a refined system that maintains high activity even when arene complexes are formed.

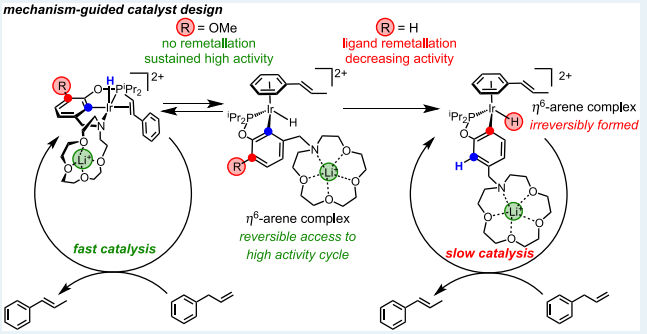

KEYWORDS: *iridium, pincer, olefin isomerization, hemilability, crown ether, pince−crown ether, switchable catalysis*

INTRODUCTION

Binding of the substrate to a transition metal center is the entry point of many catalytic cycles. While substrate binding is often a rate-limiting process, there are few methods to simply and systematically tune the rate of substrate association to the metal center.[1] Control over substrate binding therefore remains a fundamental challenge in the field of homogeneous catalysis.

One method to control substrate binding utilizes stimuli-responsive supramolecular encapsulation. External stimuli can open or close the "gate" to modulate access of the substrate to the active site.[2] Such a situation is frequently encountered in biological catalysis with allosterically modulated enzymes.[3−7] Synthetic catalysts have also been designed with artificial allosteric cofactors through elegant control of the secondary coordination sphere.[2,8−14] Other methods to control substrate binding focus on the primary coordination sphere.[1] Photochemical ligand dissociation can open a substrate binding site,[15,16] or a change in catalyst oxidation state can alter the kinetics and thermodynamics of ligand substitution.[17−20] Supporting ligands with Lewis basic sites can interact with externally added Lewis acids to modulate catalyst properties as well.[21−23]

Hemilabile ligands, which are multidentate ligands featuring both strong and weak donors, represent one opportunity to gate substrate access to a metal center via the primary coordination sphere.[1,24,25] The weak donors can be displaced by the substrate, allowing catalysis to occur, then reassociate upon dissociation of the substrate. Because the dynamic behavior of hemilabile ligands involves a delicate energetic balance, it can be difficult to tune or control hemilability.[26]

To introduce an element of tunability to hemilabile ligands, we have developed "pincer-crown ether" ligands that incorporate an aza-crown ether capable of cation binding into a pincer framework.[1,27] Substitution of a crown ether oxygen donor by a substrate is often unfavorable when no cations are present in a solution, but when cations are present, the dissociated macrocycle can be stabilized by cation−crown interactions and substrate binding becomes favorable.[28]

A remarkable degree of control over the activity of olefin isomerization is achieved when iridium(III) pincer-crown ether complexes are used in conjunction with simple alkali metal salts.[29] The cationic iridium hydride complex $[(\kappa^5\text{-}^{15c5}\text{NCOP}^{i\text{Pr}})\text{IrH}][\text{BAr}^{\text{F}}_4]$ (Ar^{F} = 3,5-bis-(trifluoromethyl)-phenyl) (**1**, Scheme 1) isomerizes allylbenzene to (*E*)-*β*-methylstyrene in dichloromethane at room temperature slowly when no salts are added (TOF = 1.8 h^{-1}). The addition of $\text{NaBAr}^{\text{F}}_4$ leads to modest rate acceleration (TOF = 5.4 h^{-1}), while the addition of $\text{LiBAr}^{\text{F}}_4\cdot 3\text{Et}_2\text{O}$ leads to more than 1000-

Received: August 30, 2020
Revised: October 9, 2020

https://dx.doi.org/10.1021/acscatal.0c03784
ACS Catal. 2020, 10, 13019−13030

Scheme 1. Cation-Enhanced Olefin Isomerization by an Iridium Pincer-Crown Ether Catalyst, Highlighting Proposed Key Intermediate A

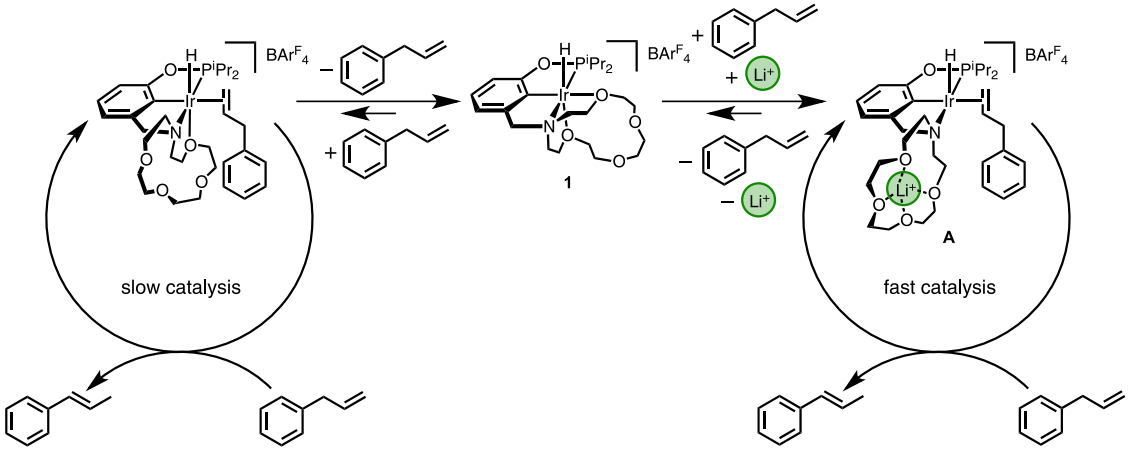

fold rate enhancements (TOF = 2750 h^{-1}).[29] The dramatic responsiveness of the catalyst to Li^+ is attributed to a significantly higher binding affinity for Li^+ based on the size of the macrocycle.[28] The tunable ether hemilability in this pincer-crown ether catalyst also renders rate enhancements reversible: catalysis can be accelerated by Li^+ ions or decelerated by the addition of chloride ions. The proposed mechanism of cation-promoted olefin isomerization is shown in Scheme 1. The iridium hydrido olefin complex **A** was proposed to be a key intermediate, motivating a search for its existence.

Here, we report the development of a pincer-crown ether olefin isomerization catalyst, guided by mechanistic studies that revealed roles of both ether and amine hemilability. *In situ* spectroscopic monitoring of olefin isomerization by **1** revealed the formation of an unknown iridium species as the reaction proceeded. The unknown species was identified as an unexpected η^6-arene complex with an altered site of metallation. Authentic synthesis of model complexes allowed full structural characterization and catalytic assessment showed poor performance. In response to this mechanistic insight, the pincer-crown ether supporting ligand backbone was synthetically modified to prevent a change in metallation. The catalyst reported here maintains high activity and exhibits improved durability under certain conditions. Additional mechanistic studies show that ether hemilability is essential for rapid isomerization, and amine hemilability (leading to η^6-arene complexes) can be tolerated—but that a change in metallation is detrimental. By directly relating catalytic activity to catalyst speciation, generally applicable insight into different modes of hemilability emerges.

RESULTS AND DISCUSSION

Spectroscopic Detection of Iridium-Containing Species During Catalysis. To search for catalytic intermediates during Li^+-promoted olefin isomerization by $[(\kappa^{5\text{-}15c5}NCOP^{iPr})IrH]^+$ (**1**), we examined allylbenzene isomerization under a range of conditions. Trace amounts of an unknown iridium-containing species, denoted **B** and identified by a characteristic hydride ^1H nuclear magnetic resonance (NMR) signal at −15.7 ppm, were observed in Li^+-containing reactions as isomerization reached completion. Monitoring reactions beyond 1 h revealed that the unknown species continued forming after isomerization was complete. The effects of Li^+ concentration, reaction temperature, and Lewis acidity of the cationic additive on the formation of **B** were examined. In all cases, unless otherwise noted, >99% yield of β-methylstyrene was observed at the end of the reaction according to NMR spectroscopy.

To examine the effect of salt concentration on catalyst speciation, the formation of **B** was monitored by NMR spectroscopy during isomerization of allylbenzene (0.75 M in CH_2Cl_2) at various $LiBAr^F_4{\cdot}3Et_2O$ concentrations. Figure 1 shows that the yield of **B** after 16 h increased markedly with increasing concentration of $LiBAr^F_4{\cdot}3Et_2O$. The trend of Figure 1 is consistent with cation binding playing a role in the formation of the unknown species.

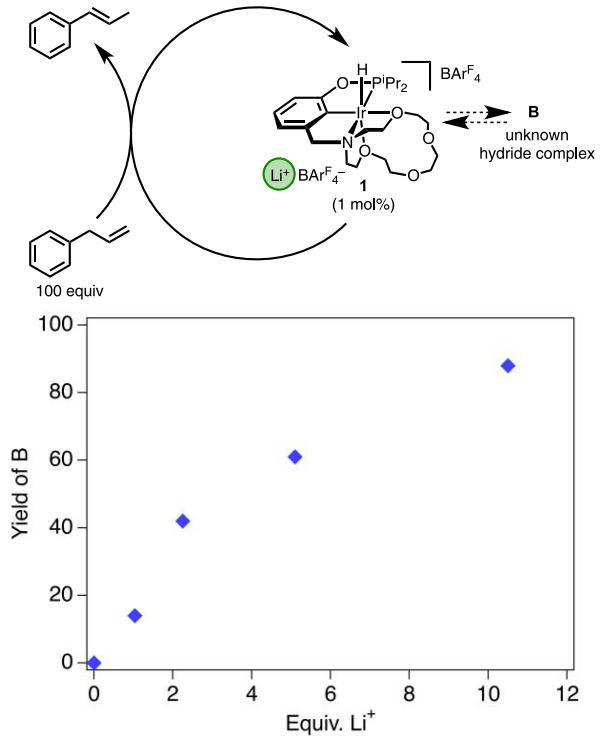

Figure 1. Plot showing Li^+ dependence of the formation of **B** during allylbenzene isomerization at room temperature (7.5 mM **1**, 0.75 M allylbenzene, 16 h).

https://dx.doi.org/10.1021/acscatal.0c03784
ACS Catal. 2020, 10, 13019−13030

To assess the influence of cation Lewis acidity on catalyst speciation, the lithium salt $LiAl(OC(CF_3)_3)_4$ was examined. Excess Et_2O has been shown to attenuate Li^+-promoted rate enhancements in olefin isomerization by pincer-crown ether catalysts,[29] leading to the hypothesis that the ether-free salt $LiAl(OC(CF_3)_3)_4$ might lead to stronger cation−crown interactions at lower salt concentrations.[30] Only 20 min after mixing catalyst **1** (7.5 mM) and 2 equiv $LiAl(OC(CF_3)_3)_4$ with allylbenzene (0.75 M) in CH_2Cl_2, complete isomerization to *β*-methylstyrene and complete conversion of **1** to **B** were observed by NMR spectroscopy. The formation of **B** thus depends on both the concentration of Li^+ salts and the Lewis acidity of the specific salt employed.

To probe the role of temperature, a reaction vessel containing 5 mM **1**, 25 mM $LiBAr^F_4{\cdot}3Et_2O$, and 0.5 M allylbenzene in CD_2Cl_2 was heated at 35 °C for 16 h. The reaction produced **B** quantitatively according to NMR spectroscopy. For comparison, allylbenzene isomerization at room temperature (20 °C) in CD_2Cl_2 under these conditions gave 61% yield of **B**. Under analogous conditions, but utilizing the higher boiling solvent 1,2-dichloroethane-d_4 and heating at 80 °C, **1** was fully converted to **B** within 1 h. These studies show that elevated temperatures increase catalyst speciation.

The catalytic runs under variable conditions provide insight into the factors that lead to a change in a catalyst state. At room temperature with $LiBAr^F_4{\cdot}3Et_2O$ and short reaction times, only trace amounts of **B** are observed. Formation of **B** increases at high $LiBAr^F_4{\cdot}3Et_2O$ concentrations and with longer reaction times. At elevated reaction temperatures or when strongly Lewis acidic Li^+ sources are used, formation of **B** is quantitative even at short reaction times. Catalyst speciation was therefore predicted to become problematic during high-temperature isomerization reactions and when strongly Lewis acidic cations are employed. In this context, it was important to fully characterize **B** and determine the extent to which it is detrimental to catalysis.

Synthesis and Characterization of Analogues of Iridium-Containing Species B. Styrene was employed as a nonisomerizable model olefin to aid in the characterization of a complex analogous to **B**. Complex **1** and 20 equiv styrene were stirred in CD_2Cl_2 for 24 h, but no reaction was observed. When 1.5 equiv $LiBAr^F_4{\cdot}3Et_2O$ was included with complex **1** and 20 equiv styrene, however, full conversion of **1** to a single new hydride-containing product was observed within 30 min (Scheme 2). The chemical shift of the hydride resonance in the product (^{1}H NMR δ −15.5) is very similar to that of **B** (^{1}H NMR δ −15.7). There is a single resonance in the ^{31}P NMR spectrum of the product (δ 161.4).

Scheme 2. Synthesis of an η^6-Styrene Iridium Complex Aided in Identification of the Unknown Species Observed in Allylbenzene Isomerization

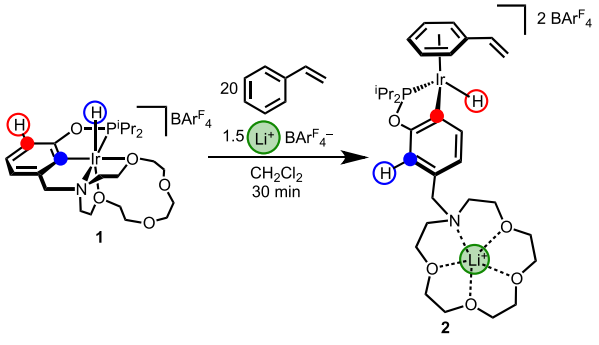

The spectroscopic data was vetted as a possible cationic hydrido η^2-alkene complex analogous to the postulated catalytic intermediate **A** (Scheme 1, above). While the vinylic resonances of η^2-alkene complexes are typically found upfield of the free olefin in the ^{1}H NMR spectrum,[31,32] the opposite trend was observed in the present case: the terminal vinylic resonances were shifted 0.43 ppm downfield of free styrene (Figure 2). On the other hand, the aromatic proton signals of the bound styrene were shifted 0.54 ppm upfield, again opposite to expectations for a styrene complex bound η^2 through the vinyl group. The styrene chemical shifts are more in line with an η^6-arene complex of iridium.[33]

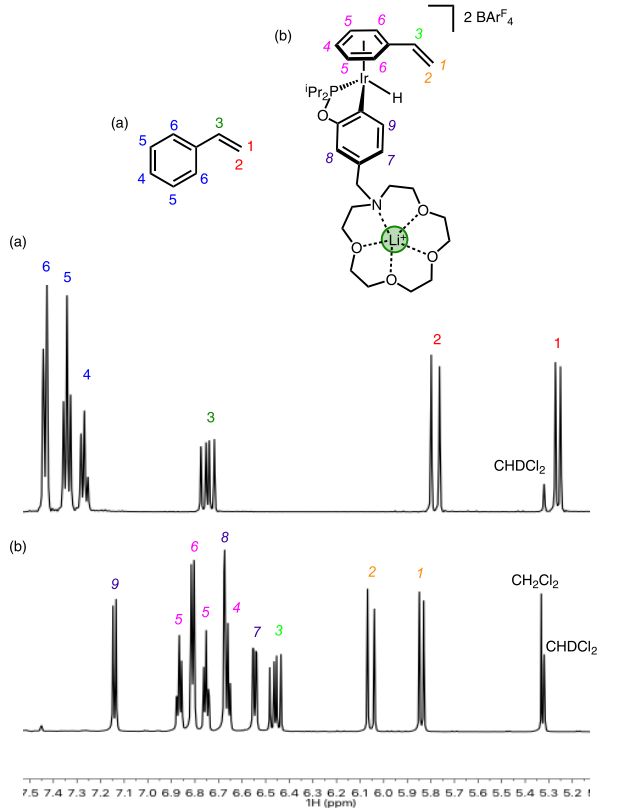

Figure 2. ^{1}H NMR spectra (downfield region) showing (a) styrene alone, and (b) an isolated sample of styrene complex **2**. Changes in the chemical shifts of the aryl and vinylic resonances of styrene aided in identification of **2** as an η^6-styrene complex.

A three-legged piano stool complex capped by η^6-styrene could form upon dissociation of the amine arm of the pincer-crown ether ligand. Significant changes in the ^{1}H NMR resonances for the aryl backbone of the pincer ligand indicated a more complex rearrangement, however. The aryl resonances for complex **1** appear as a triplet and two doublets. The aryl resonances for complex **2** appear as a doublet (J = 7.8 Hz), a doublet (J = 2.0 Hz), and a doublet of doublets (J = 7.8, 2.0 Hz). We therefore assign the species as an η^6-styrene complex in which the aryl backbone has reductively eliminated, rotated, and oxidatively added at the C−H bond ortho to the phosphinite to form $[Li@(\kappa^2\text{-}^{15c5}NC'OP^{iPr})Ir(\eta^6\text{-styrene})H]^{2+}$ (**2**, Scheme 2). Consistent with this assignment, the ^{1}H NMR resonances corresponding to the crown ether protons appear in a narrow chemical shift range, as expected for an aza-crown

https://dx.doi.org/10.1021/acscatal.0c03784
ACS Catal. 2020, 10, 13019−13030

ether lacking any amine or ether interactions with iridium.[34] We have previously observed "remetallation" from the 2-position to the 6-position of the arene backbone in stoichiometric reactivity studies of iridium(I) carbonyl pincer-crown ether complexes in the presence of Ca^{2+}.[35] Similar examples of metallation at the "wrong" position can be found in pincer complexes with phenyl backbones and nitrogen donors.[36,37] Our observations show that, under certain conditions, both ethers and amines can act as hemilabile ligands in the pincer-crown ether system, with amine dissociation sometimes leading to undesired reaction pathways.

To probe the generality of η^6-arene complex formation, cationic complex **1** was allowed to react with an electron-poor arene (naphthalene) and an electron-rich arene (mesitylene). When complex **1** was treated with 20 equiv naphthalene and 2.0 equiv $LiBAr^F_4{\cdot}3Et_2O$ in dichloromethane, full conversion to a new species was observed over 16 h. The product is spectroscopically almost identical to styrene complex **2** and is thus assigned as $[Li@(\kappa^2\text{-}^{15c5}NC'OP^{iPr})Ir(\eta^6\text{-naphthalene})\text{-}H]^{2+}$ (**3**, Scheme 3). The reaction with naphthalene proceeds

Scheme 3. Synthesis of Three η^6-Arene Iridium Complexes in Which the Pincer Ligand Has Remetallated, Giving Products with a Bidentate Ligand Binding Mode

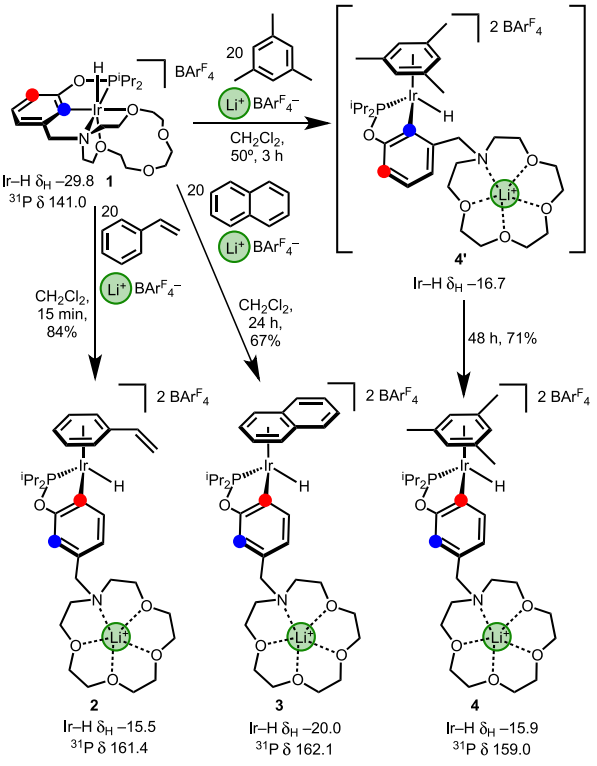

markedly more slowly than the analogous reaction with styrene (16 h vs 0.5 h). The reactivity difference is attributed to the ability of styrene to support η^2-coordination via the vinyl group before intramolecular rearrangement to an η^6-arene structure.

When mesitylene was used as the capping arene ligand, the reaction rate fell between styrene and naphthalene, and a previously unobserved intermediate appeared. The major species (77%) 3 h after treating complex **1** with 30 equiv mesitylene and 2.8 equiv $LiBAr^F_4{\cdot}3Et_2O$ in CH_2Cl_2 had a hydride resonance at −16.7 ppm, while the minor species (33%) had a hydride resonance at −15.9 ppm. Over the course of 48 h, the major hydride signal (δ −16.7) disappears completely and the minor hydride signal (δ −15.9) becomes the sole product. The aryl resonances for the ligand backbone of the intermediate species appear as a triplet and two doublets, leading us to assign this intermediate as a bidentate phenylphosphinite arene complex that has not undergone remetallation (**4′**, Scheme 3). This species is proposed to then undergo reductive elimination, rotation, and oxidative addition of the other C−H bond ortho to the phosphinite to reach the thermodynamically preferred remetallated product $[Li@(\kappa^2\text{-}^{15c5}NC'OP^{iPr})Ir(\eta^6\text{-mesitylene})H]^{2+}$ (**4**). The reaction pathway may be the same for each arene ligand, but we postulate that the electron-rich mesitylene ligand stabilizes the intermediate arene adduct more than styrene and naphthalene do,[38] slowing down remetallation relative to the other cases where no intermediate is observed.

The structural assignments of the arene complexes were confirmed by an X-ray diffraction (XRD) study on single crystals of **3**, which were grown by layering pentane onto a concentrated dichloromethane solution and allowing the solvents to mix at −30 °C. The structure unambiguously shows η^6-naphthalene binding and the pincer ligand remetallation that positions the crown ether away from the metal center (Figure 3). Crystals of **3** exhibited whole-molecule disorder, with the occupancy of the minor component ∼20% (see the Supporting Information for details).

Role of η^6-Arene Complexes in Catalysis. Based on the iridium complexes obtained using styrene, naphthalene, and mesitylene, and their spectroscopic similarity to species **B** observed in allylbenzene isomerization, **B** was assigned as the remetallated arene complex of β-methylstyrene (the product of

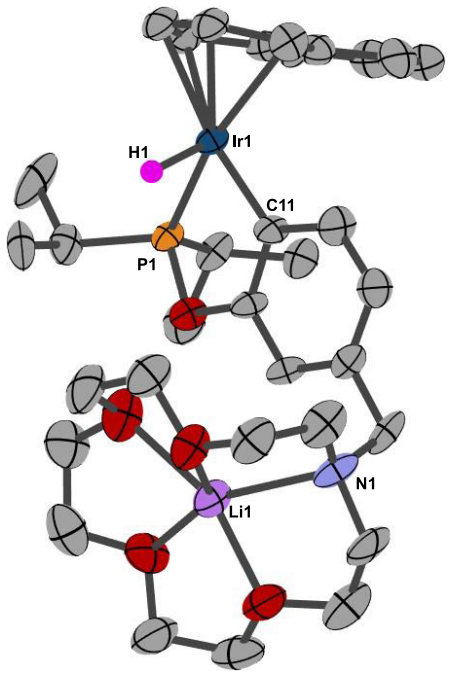

Figure 3. Structural representation of the cation of **3** with ellipsoids drawn at the 50% probability level. All hydrogen atoms except the hydride are omitted for clarity. Selected distances (Å) and angles (°): Ir1−P1 2.221(2), Ir1−C11 2.031(5), Ir1−H1 1.498, P1−Ir1−C11 78.68(14), P1−Ir1−H1 79.1, and C11−Ir1−H1 81.3.

https://dx.doi.org/10.1021/acscatal.0c03784
ACS Catal. 2020, 10, 13019−13030

allylbenzene isomerization). Formation of **B** is significantly slower than the formation of **2**, consistent with *β*-methylstyrene being released from the coordination sphere of the catalyst upon its initial formation from allylbenzene, before later coordinating in an η^6 fashion.

Observing a new complex formed during catalysis, especially one formed in increasing amounts toward the end of a catalytic run, does not necessarily implicate that species as a relevant intermediate.[39] Catalytic species **B** could be a relevant intermediate that does not build up until isomerization reaches completion, or it could be an unwanted off-cycle species. To probe this, we tested the viability of **2** as a precatalyst in allylbenzene isomerization (Scheme 4).

Scheme 4. Catalytic Allylbenzene Isomerization by the η^6-Styrene Iridium Complex 2

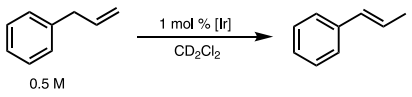

[Ir] = **1** + $LiBAr^F_4$, TOF = 1870 h^{-1}

[Ir] = **2**, TOF = 3.2 h^{-1}

Catalytic isomerization of allylbenzene (0.5 M) in CD_2Cl_2 by the Li^+-containing η^6-styrene complex **2** (5 mM) proceeded very slowly (TOF = 3.2 h^{-1}, first-order half-life $t_{1/2}$ = 20.7 h) relative to isomerization catalyzed by **1** in the presence of Li^+ (TOF = 1870 h^{-1}, zero-order half-life $^0t_{1/2}$ = 1.6 min). During isomerization by **2**, there was no hydride resonance discernible in the ^{1}H NMR spectrum, indicating that the catalyst resting state is not an iridium hydride. Upon completion of the reaction, a hydride resonance matching that of **B**, assigned as the η^6-*β*-methylstyrene adduct, was observed. On the basis of the slow rate of allylbenzene isomerization by **2**, relative to **1** in the presence of $LiBAr^F_4{\cdot}3Et_2O$, we conclude that the remetallated η^6-arene complex is not an intermediate in the fast catalytic cycle of Scheme 5.

Catalysis involving η^6-arene complexes could be slow because of unfavorable re-entry into the original catalytic cycle (requiring arene dissociation and ligand remetallation back to the original binding mode); or it could be slow because the η^6-arene complexes proceed through an independent catalytic cycle with slower individual steps. To distinguish between these possibilities, evidence for the reversibility of the ligand remetallation was sought. Styrene-d_8 (10 equiv) was added to an isolated sample of **2** in CD_2Cl_2, and the reaction was monitored by NMR spectroscopy (Scheme 6). Arene

Scheme 6. Labeling Experiment Using Styrene-d_8 to Probe Reversibility of η^6-Arene Complex Formation

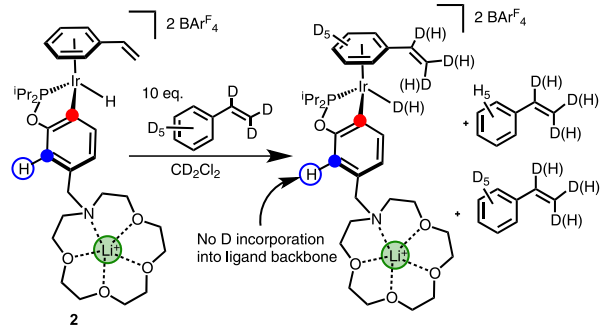

exchange occurs rapidly, as confirmed by the disappearance of resonances for bound protio styrene and the appearance of resonances assigned to free protio styrene in the ^{1}H NMR spectrum. There is also H/D scrambling of the olefinic protons of styrene, and the hydride resonance of starting complex **2** diminishes (22% hydride remains by integration) due to the formation of the corresponding iridium deuteride. There is, however, no D incorporation into the aryl backbone of the NCOP ligand. If the reductive elimination, rotation, oxidative addition pathway that leads to the formation of **2** is reversible, D incorporation would be expected at the aryl C−H bond ortho to the phosphinite in **2** (Scheme 6). We conclude from this experiment that the remetallation involved in the formation of **2** is not reversible under the reaction conditions, and therefore **2** operates via an independent catalytic cycle (Scheme 5).

The remetallated backbone of the arene complexes raised the possibility that the role of Li^+ in isomerization catalysis might be to promote remetallation to generate a highly active catalyst derived from **1**. If this were the case, however, the remetallated arene complex **2** should resemble an active

Scheme 5. Proposed Mechanism of Cation-Promoted Allylbenzene Isomerization, Including the Newly Identified η^6-Arene Complexes[a]

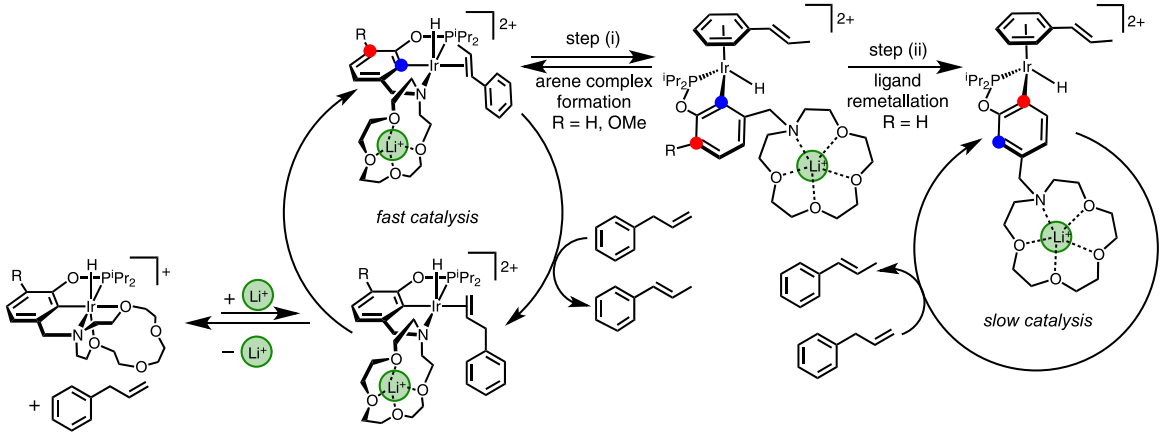

[a]A new catalyst with a methoxy substituent ortho to the phosphinite prevents remetallation and sustains catalytic activity.

https://dx.doi.org/10.1021/acscatal.0c03784
ACS Catal. 2020, 10, 13019−13030

intermediate, so the low catalytic activity of **2** helps rule out this mechanistic possibility. The η^6-arene ligand itself is also clearly not required for productive catalysis, given that 1-hexene isomerization by **1** in the presence of Li^+ was previously reported to proceed at a comparable rate to allylbenzene isomerization.[29] To further support that the role of Li^+ is not to trigger remetallation of the pincer ligand and generate a highly active, low-coordinate iridium center, a version of **1** with the site of remetallation occupied by a blocking group was prepared. If remetallation is a key step in highly active Li^+-promoted catalysis, then the new catalyst should not exhibit dramatic Li^+ enhancement since the remetallation pathway is blocked.

Synthesis and Reactivity of a "Remetallation-Proof" Catalyst. To prevent the process of remetallation observed with **1**, we turned to a pincer ligand with the site of remetallation blocked by a methoxy group, ($^{MeO\text{-}15c5}$NCOP^{iPr})-H.[40] With the methoxy group ortho to the phosphinite, the ligand presents only one possible site of metallation. We previously reported iridium carbonyl complexes with this particular pincer-crown ether ligand,[40] but the carbonyl-free analogue of **1** has not been reported.

Allowing the ligand ($^{MeO\text{-}15c5}$NCOP^{iPr})H to react with $[Ir(COD)Cl]_2$ (COD = 1,5-cyclooctadiene) yielded (κ^4-$^{MeO\text{-}15c5}$NCOP^{iPr})Ir(H)(Cl) (**5**, Scheme 7). Single crystals

Scheme 7. Synthesis of an Iridium Pincer-Crown Ether Catalyst with a Modified Ligand Backbone

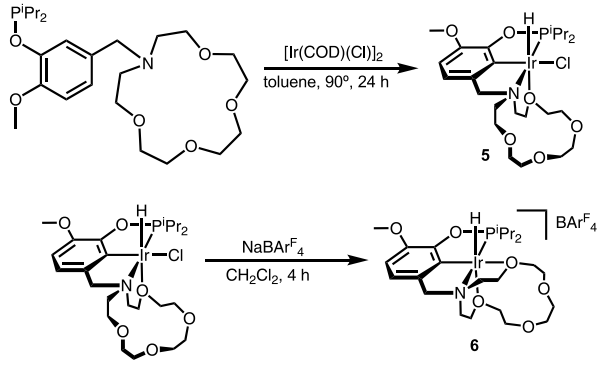

of **5** suitable for an X-ray diffraction study (XRD) were grown from a dichloromethane solution layered with pentane (Figure 4). Comparing the crystallographic parameters of **5** with the previously reported complex (κ^4-^{15c5}NCOP^{iPr})Ir(H)(Cl), which has no methoxy group ortho to the phosphinite, reveals no significant differences between the two in the primary coordination sphere of iridium. Chloride abstraction with $NaBAr^F_4$ provided the cationic complex [(κ^5-$^{MeO\text{-}15c5}$NCOP^{iPr})-IrH]$^+$ (**6**, Scheme 7).

The ability of methoxy-containing complex **6** to bind arenes in an η^6 fashion was examined using styrene and mesitylene. Treating complex **6** with styrene in the presence of 1.5 equiv $LiBAr^F_4{\cdot}3Et_2O$ did not lead to any observed reaction after 30 min. This draws a sharp contrast to complex **1**, which undergoes quantitative conversion to η^6-arene complex **2** under the same conditions, as described above. When **6** was treated with the more electron-rich arene mesitylene under otherwise identical conditions, the "normally metallated" arene complex was generated in 22% yield in 30 min according to ^{1}H NMR spectroscopy. After 72 h, the yield of arene complex was 63%. The ^{31}P NMR spectrum also reflects arene complex

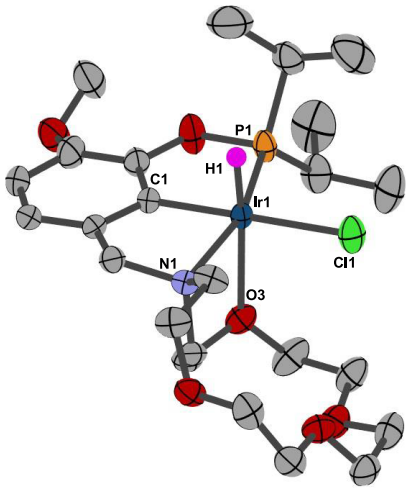

Figure 4. Structural representation of **5** with ellipsoids drawn at the 50% probability level. All hydrogen atoms except the hydride are omitted for clarity. Selected distances (Å) and angles (°): Ir1−P1 2.1861(7), Ir1−O3 2.352(2), Ir1−C1 1.974(3), Ir1−N1 2.235(2), and Ir1−Cl1 2.4496(8); P1−Ir1−O3 100.13(6), O3−Ir1−Cl1 94.96(6), C1−Ir1−O3 87.81(10), C1−Ir1−Cl1 173.90(9), and N1−Ir1−O3 78.24(8).

formation, with peaks corresponding to **6** (δ 142.4) and an η^6-arene complex (δ 151.2), which matched the ratio of products based on the integration of the hydride resonances. Interestingly, when the same reaction was run using $LiAl(OC(CF_3)_3)_4$ instead of $LiBAr^F_4{\cdot}3Et_2O$, the η^6-mesitylene adduct was generated in 73% yield in just 30 min, according to ^{1}H NMR spectroscopy. This result is attributed to the higher Lewis acidity of Li^+ in the ether-free salt $LiAl(OC(CF_3)_3)_4$ compared to $LiBAr^F_4{\cdot}3Et_2O$. While attempts to isolate this normally metallated arene complex were unsuccessful, the spectroscopic data are consistent with arene complexation without remetallation in the formation of [Li@(κ^2-$^{MeO\text{-}15c5}$NCOP^{iPr})Ir(η^6-mesitylene)H]$^{2+}$.

The need for electron-rich arenes to induce arene binding by complex **6** suggests that these arene complexes are less stable than the remetallated arene complexes produced from **1**. The thermodynamic preference for remetallation could avoid steric interactions between the arene ligand and the pendant aza-crown ether moiety, or it could minimize electrostatic repulsion between the cationic iridium center and Li^+ encapsulated in the crown and their respective counteranions. The reactivity of complex **6** enabled us to pose the question of whether the low activity of complex **2** was due to the presence of an η^6-arene ligand or due to the remetallation of the pincer backbone. Complex **6** was therefore examined for allylbenzene isomerization.

Catalytic Activity of the "Methoxy-Blocked" Complex 6. The new cationic iridium hydride complex **6** was compared with original catalyst **1** to understand the impact of remetallation on isomerization catalysis. Under standard conditions of 1 mol % catalyst (0.5 M substrate, 5 mM catalyst) in the presence of 1 equiv $LiBAr^F_4{\cdot}3Et_2O$, both **1** and **6** isomerize allylbenzene to β-methylstyrene in less than 10 min at 25 °C with high stereoselectivity (98:2 E:Z). The Ir/Li^+ systems are among the most highly active isomerization catalysts known.[41−45] For comparison, other iridium catalysts require high temperatures (70−125 °C) to efficiently isomerize terminal olefins to internal positions.[43,46−48]

https://dx.doi.org/10.1021/acscatal.0c03784
ACS Catal. 2020, 10, 13019−13030

Even when the catalyst loading of **1** or **6** was lowered to 0.2 mol % (0.5 M substrate, 1 mM catalyst, 5 mM $LiAl(OC(CF_3)_3)_4$) and the reaction was heated at 70 °C in 1,2-DCE-d_4, the isomerization activity was similar for the two catalysts (Scheme 8). *In situ* monitoring of the catalyst speciation by

Scheme 8. Comparisons of Olefin Isomerization by 1 and the Methoxy-Blocked Catalyst 6

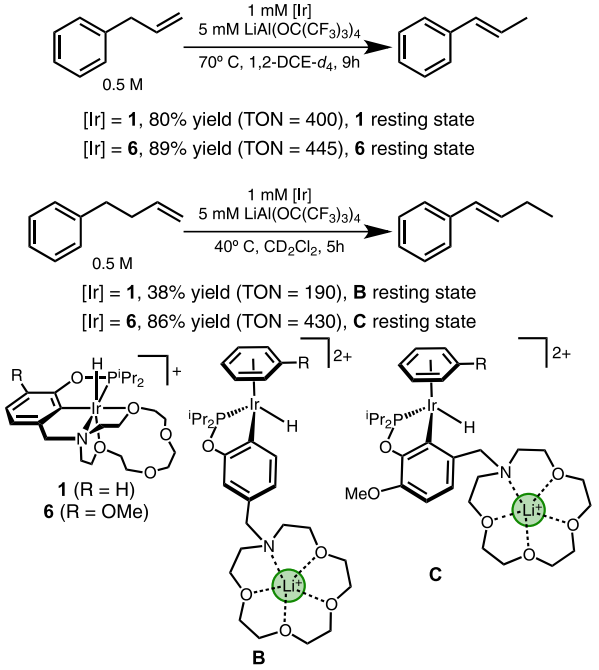

NMR spectroscopy revealed that, under these conditions, the resting state during catalysis was the starting catalyst (**1** or **6**). These studies show that during allylbenzene isomerization, the resting state is the starting catalysts; conversion to arene complexes **B** or **C** only occurs after all allylbenzene is consumed. The mechanistic implications of this are discussed below.

Because catalyst **1** is converted to a new species at the conclusion of the isomerization, the performance differs markedly when attempting to recycle the catalyst. As shown in Scheme 9, the two iridium catalysts (5 mM) were stirred in CD_2Cl_2 containing allylbenzene (0.5 M) and $LiAl(OC(CF_3)_3)_4$ (10 mM) for 20 min at 25 °C before ^{1}H NMR spectroscopic analysis revealed complete conversion to *β*-

Scheme 9. Comparison of the Recyclability of Catalysts 1 and 6 in Multiple Allylbenzene Isomerization Reactions

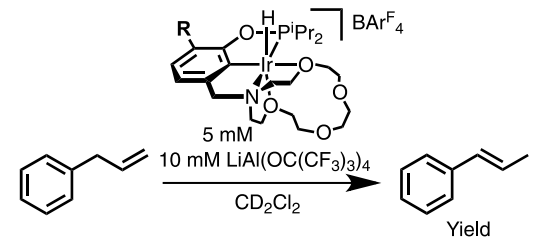

Substrate additions	Yield Reaction A R = H	Yield Reaction B R = OMe
100 equiv, 20 min	100%	100%
+100 equiv, 40 min	10%	100%
+100 equiv, 80 min	7%	75%

methylstyrene. At the conclusion of the reaction, the speciation in reaction A shifted from catalyst **1** to an η^6-arene complex with a remetallated phenyl backbone (species **B** in Scheme 8), while the speciation in reaction B shifted from **6** to an η^6-arene complex with the original metallation position (species **C** in Scheme 8). The distinct speciation in each reaction was reflected in distinct reactivity when a second aliquot of allylbenzene was added and the reaction was allowed to proceed for 40 min, with reaction A (with the remetallated catalyst) giving 10% yield and reaction B (original metallation position) giving 100% yield. After allowing both reactions to proceed to completion, a third aliquot was added and the reaction stirred for 80 min, resulting in 75% conversion for reaction B and only 7% conversion for reaction A. The methoxy-blocked catalyst **6** gives higher yields than the original catalyst under these recycle conditions. This comparison reveals that the formation of an arene complex does not inherently deactivate the catalyst, but that remetallation is the key process leading to lower activity.

A more challenging substrate, 4-phenyl-1-butene, was examined next. Access to the thermodynamically favored isomer, 1-phenyl-1-butene, requires two positional isomerizations. At a low 0.2 mol % catalyst loading (0.5 M substrate, 1 mM catalyst, 5 mM $LiAl(OC(CF_3)_3)_4$) at 40 °C in CD_2Cl_2, catalyst **6** produced 1-phenyl-1-butene in 86% yield (TON = 430) after 5 h. The original catalyst **1** only gave 38% yield (TON = 190) under the same conditions. In contrast to the isomerization of allylbenzene, the resting states during both **1**- and **6**-catalyzed isomerization of 4-phenyl-1-butene are arene complexes under these conditions (Scheme 8). However, only catalyst **1** undergoes remetallation during the isomerization, leading to lower activity for this more challenging substrate.

The comparative catalysis studies show that catalyst **6** exhibits markedly higher activity than **1** for a challenging substrate requiring multiple isomerizations, or when the catalyst is recycled in multiple runs. In addition to demonstrating the superior performance of **6** under certain conditions, the comparisons provide important mechanistic insights. Scheme 5 (above) shows the catalytic cycle proposed for allylbenzene isomerization. The collection of studies is consistent with binding of the terminal olefin allylbenzene occurring faster than amine labilization and arene complex formation, while binding of an internal olefin is slower than amine labilization and arene complex formation. Thus, no change in resting state is observed during allylbenzene isomerization, but once all of the allylbenzene is consumed only internal olefin remains; the catalyst converts to arene complexes. This leads to lower activity for catalyst **1** in recycling experiments. When multiple isomerizations are required, as in 4-phenyl-1-butene isomerization, all of the terminal olefin is consumed before the reaction is complete. The mechanism proposed in Scheme 10 illustrates how the arene complexes become the resting states during the reaction because the rate of internal olefin substitution is slower than the rate of arene complex formation, k_a (internal) < k_{arene}. The arene complexes derived from catalysts **1** and **6** have very different activity. Catalyst **1** loses almost all activity upon arene complex formation because irreversible remetallation to a different position of the pincer backbone occurs. Catalyst **6** does not remetallate and retains high activity, presumably because it can readily re-enter the original rapid catalytic cycle from the η^6-arene complex **C** (Scheme 8 and Scheme 10). A

https://dx.doi.org/10.1021/acscatal.0c03784
ACS Catal. 2020, 10, 13019−13030

Scheme 10. Proposed Mechanism of 4-Phenyl-1-Butene Isomerization Highlighting Change in Resting State to Arene Complexes Because k_a (internal) Is Smaller than k_{arene}

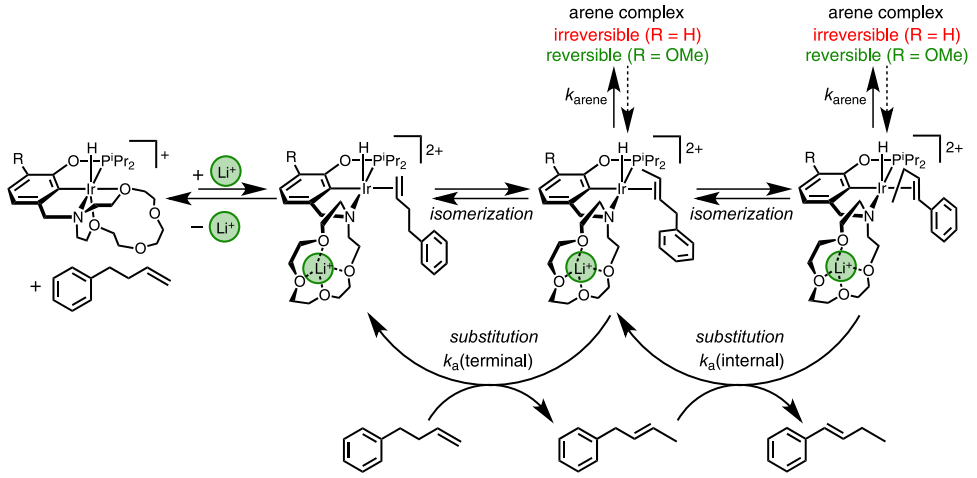

simple modification of the ligand backbone thus prevents significant losses in catalyst activity under certain conditions.

CONCLUSIONS

Mechanistic studies of cation-promoted olefin isomerization by iridium pincer-crown ether complexes reveal unexpected deactivation pathways. In the original catalyst structures, amine dissociation leads to metallation at a different position on the aryl backbone of the pincer and formation of an η^6-arene complex with very low activity. Access to the off-cycle species is promoted by high concentrations of Li^+, high temperatures, and long reaction times. To block remetallation, a methoxy group was installed in the pincer backbone. Under forcing conditions, arene complexes are still observed for the new catalyst **6**, yet ≥75% yields of internal olefin are still obtained.

The present study provides insight into the opportunities and challenges associated with tunable hemilability. The cationic iridium hydride catalyst **1** features a macrocycle with the amine and two ethers bound. Labilizing the ethers through cation−crown interactions is critical to achieving high activity in this system. Labilizing the amine, however, can lead to reductive elimination and metallation at a different position on the aryl backbone. Amine hemilability is not inherently problematic, however, as long as remetallation is prevented.

EXPERIMENTAL SECTION

General Considerations. All manipulations were performed using standard Schlenk and glovebox techniques under a N_2 atmosphere. NMR-scale reactions were prepared under N_2 and monitored in Teflon-sealed tubes. Pentane, diethyl ether, toluene, and benzene were used in a glovebox without purging, such that traces of those solvents were present in the atmosphere and in the solvent bottles. Tetrahydrofuran was actively avoided due to its ability to replace the Et_2O donors in $LiBAr^F_4{\cdot}3Et_2O$, making the Li^+ cation less Lewis acidic. ^1H, $^{31}P\{^1H\}$, $^{19}F\{^1H\}$, and $^{13}C\{^1H\}$ spectra were recorded on 500 or 600 MHz spectrometers at 298 K. NMR solvents were purchased from Cambridge Isotope Laboratories, Inc., and were freeze−pump−thaw degassed three times before drying via passage over activated alumina and storage over 3 Å molecular sieves. ^1H and ^{13}C chemical shifts are reported in ppm relative to residual protio solvent resonances. $^{31}P\{^1H\}$ chemical shifts are reported via absolute referencing to the corresponding ^1H spectra. The compounds (^{15c5}NCOP^{iPr})Ir(H)(Cl),[49] [(^{15c5}NCOP^{iPr})IrH][BAr$_4^F$] (**1**),[49] ($^{MeO\text{-}15c5}$NCOP^{iPr}),[40] $LiBAr^F_4{\cdot}3Et_2O$,[50] and $LiAl(OC(CF_3)_3)_4$[51] were prepared according to literature procedures. Some $NaBAr^F_4$ was purchased from Matrix Scientific and purified by crystallization and rigorous drying prior to use,[52] and some $NaBAr^F_4$ was synthesized according to literature protocol.[53] Allylbenzene, 4-phenyl-1-butene, styrene, and mesitylene were freeze−pump−thaw degassed three times before drying via passage over a small column of activated alumina and storage over 3 Å molecular sieves. All other reagents were commercially available and used without further purification. Elemental analyses were performed by Robertson Microlit Labs (Ledgewood, NJ). High-resolution mass spectrometry was carried out with a Q Exactive HF-X (ThermoFisher, Bremen, Germany) mass spectrometer. Samples in dichloromethane were introduced via a heated electrospray source (HESI) at a flow rate of 10 μL/min. Xcaliber (ThermoFisher) was used to analyze the data. Single-crystal X-ray diffraction data was collected on a Bruker APEX-II CCD diffractometer at either 150 or 273 K with Cu Kα radiation.

Synthesis of [Li@(κ^2-^{15c5}NC′OP^{iPr})Ir(η^6-styrene)H][BAr$^F_4$]$_2$ (2). In a glovebox, a 20 mL scintillation vial was charged with 0.2137 g (0.1428 mmol) of **1** and 0.2330 g (0.2134 mmol) $LiBAr^F_4{\cdot}3Et_2O$. The solids were dissolved in 8 mL of CH_2Cl_2 and 0.328 mL of styrene (2.853 mmol, 20 equiv) was added, resulting in a color change of the solution from yellow-orange to bright red. The solution was stirred for 15 min, then the solvent was removed under vacuum, and the resulting orange solid was washed thoroughly with pentane. The solid was dissolved in dichloromethane (8 mL), pentane was layered onto the concentrated solution, and the solvents were allowed to mix at −30 °C, yielding 0.3229 g of yellow crystalline solid (**2**, 84%). The material was 99% pure by NMR spectroscopy. ^1H NMR (600 MHz, CD_2Cl_2): δ 7.75 (s, 16H, BAr*H*), 7.59 (s, 8H, BAr*H*), 7.14 (d, *J* = 7.9 Hz, 1H, Ar*H*), 6.87 (t, *J* = 6.3 Hz, 1H, styrene-Ar*H*), 6.81 (d, *J* = 7.0 Hz, 2H, styrene-Ar*H*), 6.75 (t, *J* = 6.3 Hz, 1H, styrene-Ar*H*), 6.68 (d, *J* = 2.0 Hz, 1H, Ar*H*), 6.66 (t, *J* = 6.2 Hz, 1H, styrene-Ar*H*), 6.55 (dd, *J* = 7.8, 2.0 Hz, 1H, Ar*H*), 6.46 (dd, *J* = 17.3, 10.9 Hz, 1H, styrene-C*H*CH$_2$), 6.05 (d, *J* = 17.3 Hz, 1H, styrene-CHC*H*$_2$), 5.84 (d, *J* = 11.0 Hz, 1H, styrene-CHC*H*$_2$), 3.60 (m,

https://dx.doi.org/10.1021/acscatal.0c03784
ACS Catal. 2020, 10, 13019−13030

18H, crown-CH_2 and Ar(CH_2)N), 2.64 (bs, 4H, crown-(CH_2)N(CH_2)), 2.53 (sep, J = 6.8 Hz, 1H, CH(CH$_3$)$_2$), 2.26 (sd, J = 7.3, 2.5 Hz, 1H, CH(CH$_3$)$_2$), 1.23 (dd, J = 15.9, 7.0 Hz, 3H, CH(CH_3)$_2$), 1.03 (dd, J = 17.6, 7.2 Hz, 3H, CH(CH_3)$_2$), 0.95 (dd, J = 15.4, 7.1 Hz, 3H, CH(CH_3)$_2$), 0.91 (dd, J = 12.0, 6.7 Hz, 3H, CH(CH_3)$_2$), and −15.50 (d, J = 29.6 Hz, 1H, IrH). ^{13}C NMR (151 MHz, CD_2Cl_2): δ 162.17 (q, $^1J_{BC}$ = 49.6 Hz, B-C_{Ar}), 141.05 (C_{Ar}), 135.23 (C_{BAr}), 129.30 (q, $^2J_{FC}$ = 31.4 Hz, C_{BAr}-CF_3), 128.64 (styrene-$CHCH_2$), 127.22 (styrene-CHCH_2), 125.77 (C_{Ar}), 125.02 (q, $^1J_{FC}$ = 272.6 Hz, BAr-CF_3), 120.55 (C_{Ar}), 117.93 (sept, J = 4.1 Hz, C_{BAr}), 112.47 (d, J = 12.0 Hz, C_{Ar}), 111.14 (d, J = 6.2 Hz, C_{Ar}), 103.36 (d, J = 3.4 Hz, styrene-C_{Ar}), 101.79, (styrene-C_{Ar}), 98.88 (d, J = 3.4 Hz, styrene-C_{Ar}), 98.70 (styrene-C_{Ar}), 97.90 (styrene-C_{Ar}), 68.03 (crown-CH_2), 67.82 (crown-CH_2), 67.46 (crown-CH_2), 66.74 (crown-CH_2), 58.62 (Ar(CH_2)N), 51.25 (crown-(CH_2)-N(CH_2)), 33.64 (d, $^1J_{PC}$ = 36.6 Hz, CH(CH$_3$)$_2$), 28.80 (d, $^1J_{PC}$ = 46.9 Hz, CH(CH$_3$)$_2$), 17.42 (CH(CH_3)$_2$), 17.16 (d, J = 2.6 Hz, CH(CH_3)$_2$), 16.23 (d, $^2J_{PC}$ = 5.8 Hz, CH(CH_3)$_2$), and 16.13 (d, $^2J_{PC}$ = 4.8 Hz, CH(CH_3)$_2$). ^{31}P{^{1}H} NMR (243 MHz, CD_2Cl_2): δ 161.43. HRMS: m/z calcd for ($\mathbf{2}^{2+}$) 372.655, found m/z 372.65183. Anal. calcd for $C_{95}H_{72}B_2F_{48}IrLiNO_5P$: C, 46.17; H, 2.94; N, 0.57. Found: C, 45.86; H, 2.31; N, 0.62.

Synthesis of [Li@(κ^2-^{15c5}NC′OP^{iPr})Ir(η^6-naphthalene)-H][BAr$^F_4$]$_2$ (3). In the glovebox, a 20 mL scintillation vial was charged with 0.2304 g (0.1539 mmol) of **1**, 0.3455 g (0.3164 mmol) of LiBAr$^F_4$·3Et$_2$O, and 0.4545 g (3.545 mmol, 20 equiv) of naphthalene. The solids were dissolved in CH_2Cl_2 (8 mL) and allowed to stir for 24 h, during which time the solution changed from yellow-orange to bright yellow. The solvent was removed under vacuum, and the resulting yellow solid was washed thoroughly with pentane. The crude product was then crystallized by layering pentane onto a concentrated dichloromethane solution and allowing the solvents to mix at −30 °C, yielding 0.2802 g of yellow crystalline solid (**3**, 67%). The material was 85% pure by NMR spectroscopy. ^{1}H NMR (600 MHz, CD_2Cl_2): δ 7.94 (ddd, J = 8.2, 6.2, 2.2 Hz, 1H, $C_{10}H_8$), 7.87 (m, 2H, $C_{10}H_8$), 7.78 (d, J = 8.0 Hz, 1H, $C_{10}H_8$), 7.76 (s, 16H, BArH), 7.59 (s, 8H, BArH), 7.51 (d, J = 7.0 Hz, 1H, $C_{10}H_8$), 7.43 (d, J = 8.0 Hz, 1H, ArH) 7.02 (dd, J = 11.7, 5.8 Hz, 2H, $C_{10}H_8$), 6.56 (m, 3H, ArH and $C_{10}H_8$), 3.66 (s, 4H, crown-CH_2), 3.57 (m, 12H, crown-CH_2), 2.62 (s, 4H, crown-(CH_2)N(CH_2)) 2.50 (sept, J = 7.1 Hz, 1H, CH(CH$_3$)$_2$), 1.95 (m, 1H, CH(CH$_3$)$_2$), 1.10 (dd, J = 15.6, 6.9 Hz, 3H, CH(CH_3)$_2$), 1.03 (dd, J = 21.3, 6.9 Hz, 3H, CH(CH_3)$_2$), 0.91 (dd, J = 18.9, 6.6 Hz, 3H, CH(CH_3)$_2$), −0.03 (dd, J = 17.6, 7.2 Hz, 3H, CH(CH_3)$_2$), and −20.00 (d, J = 25.1 Hz, 1H, IrH). ^{13}C NMR (151 MHz, CD_2Cl_2): δ 162.17 (q, $^1J_{BC}$ = 49.6 Hz, B-C_{Ar}), 142.70 (C_{Ar}), 135.41 (d, J = 9.6, $C_{10}H_8$), 135.22 (C_{BAr}), 129.29 ($^2J_{FC}$ = 31.4 Hz, C_{BAr}-CF_3), 128.45 ($C_{10}H_8$), 126.31 ($C_{10}H_8$) 125.79 (C_{Ar}), 125.01 (q, $^1J_{FC}$ = 272.1 Hz, BAr-CF_3), δ 117.93 (sept, J = 4.0 Hz, C_{BAr}), 112.26 (d, J = 11.7 Hz, C_{Ar}), 104.28 (d, J = 7.5 Hz, $C_{10}H_8$), 99.13 (d, J = 6.2 Hz, C_{Ar}), 94.53 ($C_{10}H_8$), 91.66 ($C_{10}H_8$), 67.99 (crown-CH_2), 67.79 (crown-CH_2), 67.44 (crown-CH_2), 66.72 (crown-CH_2), 66.70 (crown-CH_2), 58.64 (Ar(CH_2)N), 51.26 (d, J = 5.7 Hz, crown-(CH_2)N(CH_2)), 34.87 (d, $^1J_{PC}$ = 35.3 Hz, CH(CH$_3$)$_2$), 28.05 (d, $^1J_{PC}$ = 47.6 Hz, CH(CH$_3$)$_2$), 17.50 (d, J = 2.3 Hz, CH(CH_3)$_2$), 16.31 (d, $^2J_{PC}$ = 6.2 Hz, CH(CH_3)$_2$), 16.13 (CH(CH_3)$_2$), and 15.88 (d, $^2J_{PC}$ = 5.7 Hz, CH(CH_3)$_2$). ^{31}P{^{1}H} NMR (243 MHz, CD_2Cl_2): δ 162.05. HRMS: m/z calcd for ($\mathbf{3}^{2+}$ − Li$^+$ − $C_{10}H_8$) 634.23, found m/z 634.22777. Anal. calcd for $C_{97}H_{72}B_2F_{48}IrLiNO_5P$: C, 46.69; H, 2.91; N, 0.56. Found: C, 46.43; H, 2.08; N, 0.63.

Synthesis of [Li@(κ^2-^{15c5}NC′OP^{iPr})Ir(η^6-mesitylene)H]-[BAr$^F_4$]$_2$ (4). In the glovebox, a 150 mL Teflon-sealed reaction vessel was charged with 0.2425 g (0.1620 mmol) of **1**, 0.3537 g (0.3239 mmol) LiBAr$^F_4$·3Et$_2$O, and 0.451 mL (3.242 mmol, 20 equiv) of mesitylene in 15 mL of CH_2Cl_2. The flask was brought out of the glovebox and heated at 50 °C for 48 h. No significant color change was observed. The solvent was removed under vacuum, and the resulting orange solid was washed thoroughly with pentane in the glovebox. Multiple crystallization attempts were unsuccessful so **4** was isolated and characterized as a crude orange solid (0.3188 g, 71% yield) The material was 89% pure by NMR spectroscopy. ^{1}H NMR (600 MHz, CD_2Cl_2): δ 7.75 (s, 16H, BArH), 7.59 (s, 8H, BArH), 7.09 (d, J = 7.4 Hz, 1H, ArH), 6.66 (d, J = 1.2 Hz, 1H, ArH), 6.62 (dd, J = 7.8, 1.8 Hz, 1H, ArH), 6.30 (s, 3H, mesitylene-ArH), 3.69 (s, 4H, crown-CH_2), 3.60 (m, 8H, crown-CH_2), 3.54 (s, 4H, crown-CH_2), 2.65 (m, 4H, crown-(CH_2)N(CH_2)) 2.57 (s, 9H, mesitylene-CH_3), 2.52 (m, 1H, CH(CH$_3$)$_2$), 2.08 (m, 1H, CH(CH$_3$)$_2$), 1.29 (dd, J = 15.5, 7.3 Hz, 3H, CH(CH_3)$_2$), 1.00 (dd, J = 17.3, 6.8 Hz, 3H, CH(CH_3)$_2$), 0.94 (dd, J = 17.3, 7.5 Hz, 3H, CH(CH_3)$_2$), 0.87 (dd, J = 18.3, 7.0 Hz, 3H, CH(CH_3)$_2$), and −15.87 (d, J = 30.2 Hz, 1H, IrH). ^{13}C NMR (151 MHz, CD_2Cl_2): δ 162.15 (q, $^1J_{BC}$ = 49.9 Hz, B-C_{Ar}), 140.41 (C_{Ar}), 135.21 (C_{BAr}), 129.28 (q, $^2J_{FC}$ = 31.4 Hz), 125.95 (C_{Ar}), 125.01 (q, $^1J_{FC}$ = 272.2 Hz, BAr-CF_3), 123.48 (d, J = 2.1 Hz, C_{Ar}), 117.91 (sept, J = 4.0 Hz, C_{BAr}), 112.02 (C_{Ar}), 98.31 (d, J = 2.7 Hz, mesitylene-C_{Ar}), 68.02 (crown-CH_2), 67.82 (crown-CH_2), 67.44 (crown-CH_2), 66.78 (crown-CH_2), 58.72 (Ar(CH_2)N), 51.29 (crown-(CH_2)-N(CH_2)), 31.71 (d, $^1J_{PC}$ = 36.1 Hz, CH(CH$_3$)$_2$), 28.73 (d, $^1J_{PC}$ = 48.1 Hz, CH(CH$_3$)$_2$), 20.00 (mesitylene-CH_3), 17.69 (CH(CH_3)$_2$), 17.41 (d, J = 2.2 Hz, CH(CH_3)$_2$), 15.72 (d, $^2J_{PC}$ = 6.8 Hz, CH(CH_3)$_2$), and 15.59 (d, $^2J_{PC}$ = 6.0 Hz, CH(CH_3)$_2$). ^{31}P{^{1}H} NMR (243 MHz, CD_2Cl_2): δ 159.02. HRMS: m/z calcd for ($\mathbf{4}^{2+}$ − Li$^+$ + H$^+$) 377.6640 found m/z 377.66448. Anal. calcd for $C_{96}H_{76}B_2F_{48}IrLiNO_5P$: C, 46.36; H, 3.08; N, 0.56. Found: C, 45.74; H, 2.55; N, 0.73.

Synthesis of (κ^4-$^{MeO\text{-}15c5}$NCOP^{iPr})Ir(H)(Cl) (5). A 250 mL Teflon-sealed pressure vessel was charged with 0.4140 g (0.6163 mmol) of [Ir(COD)(Cl)]$_2$, 0.5960 g (1.264 mmol) of ($^{MeO\text{-}15c5}$NCOP^{iPr})H and 50 mL of toluene. The flask was heated with stirring for 16 h at 90 °C, during which time the color of the solution changed from bright red to bright yellow. The reaction volume was reduced to ca. 20 mL under vacuum, and the concentrated solution was layered with an excess of pentane, giving bright yellow crystals of **5** (0.6230 g, 72% yield). The material was found to be analytically pure. ^{1}H NMR (600 MHz, CD_2Cl_2): δ 6.51 (d, J = 8.1 Hz, 1H, ArH), 6.34 (d, J = 8.1 Hz, 1H, ArH), 4.92 (t, J = 11.0 Hz, 1H, crown-CH_2), 4.84 (m, 1H, crown-CH_2), 4.39 (m, 2H, Ar(CH_2)N), 4.24 (dd, J = 12.9, 11.6 Hz, 1H, crown-CH_2), 4.07 (m, 2H, crown-CH_2), 3.91 (dd, J = 12.6, 10.2 Hz, 1H, crown-CH_2), 3.77 (m, 3H, crown-CH_2), 3.76 (s, 3H, Ar(OCH_3)), 3.69 (d, J = 8.0 Hz, 2H, crown-CH_2), 3.63 (m, 4H, crown-CH_2), 3.49 (d, J = 11.2 Hz, 1H, crown-CH_2), 3.45 (d, J = 10.0 Hz, 1H, crown-CH_2), 3.37 (dd, J = 11.1, 1.7 Hz, 1H, crown-CH_2), 3.22 (dd, J = 15.0, 3.1 Hz, 1H, crown-CH_2), 2.91 (d, J = 14.2 Hz, 1H, crown-CH_2), 2.54 (m, 1H, CH(CH$_3$)$_2$), 2.37 (sept, J = 6.8 Hz, 1H, CH(CH$_3$)$_2$), 1.42 (dd, J = 17.0, 7.6 Hz, 3H, CH(CH_3)$_2$), 1.37 (dd, J = 13.7, 7.2 Hz, 3H, CH(CH_3)$_2$), 1.13 (dd, J = 18.8,

https://dx.doi.org/10.1021/acscatal.0c03784
ACS Catal. 2020, 10, 13019−13030

7.0 Hz, 3H, $CH(CH_3)_2$), 0.82 (dd, J = 15.4, 6.8 Hz, 3H, $CH(CH_3)_2$), and −31.33 (d, J = 25.7 Hz, 1H, IrH). $^{13}C\{^1H\}$ NMR (151 MHz, CD_2Cl_2): δ 151.35 (d, J = 4.0 Hz, C_{Ar}), 142.84 (d, J = 12.2 Hz, C_{Ar}), 141.00 (d, J = 3.6 Hz, C_{Ar}), 136.26 (d, J = 3.8 Hz, C_{Ar}), 113.59 (s, C_{Ar}), 107.49 (s, C_{Ar}), 76.42 (s, crown-CH_2), 73.82 (s, crown-CH_2), 73.06 (s, crown-CH_2), 72.54 (s, crown-CH_2), 70.82 (d, J = 23.1 Hz, crown-CH_2), 69.79 (s, Ar(CH_2)N), 69.35 (s, crown-CH_2), 67.50 (d, J = 1.8 Hz, crown-CH_2), 64.86 (s, Ar-(OCH_3)), 63.22 (d, J = 2.3 Hz, crown-CH_2), 56.34 (s, crown-CH_2), 31.89 (d, J = 34.1 Hz, $CH(CH_3)_2$), 29.71 (d, J = 40.2 Hz, $CH(CH_3)_2$), 17.62 (s, $CH(CH_3)_2$), 17.46 (d, J = 8.0 Hz, $CH(CH_3)_2$), 17.07 (d, J = 4.7 Hz, $CH(CH_3)_2$), and 16.50 (d, J = 3.6 Hz, $CH(CH_3)_2$). $^{31}P\{^1H\}$ NMR (202 MHz, CD_2Cl_2): δ 144.21. HRMS: m/z calcd for (**5** − Cl^-) 664.24, found m/z 664.23566. Anal. calcd for $C_{24}H_{42}ClIrNO_6P$: C, 41.23; H, 6.05; N, 2.00. Found: C, 41.42; H, 5.63; N, 1.99.

Synthesis of [(κ^5-$^{MeO\text{-}15c5}$NCOP^{iPr})IrH][BAr^F_4] (6). In a glovebox, a 20 mL scintillation vial was charged with 0.6230 g (0.8910 mmol) of (κ^4-$^{MeO\text{-}15c5}$NCOP^{iPr})Ir(H)(Cl) (**5**) and 0.8650 g (0.9761 mmol) of $NaBAr^F_4$. The solids were dissolved in 15 mL of CH_2Cl_2 and allowed to stir for 3 h, during which time the solution changed from bright yellow to orange. The mixture was filtered over a short column of activated alumina; then, the solvent was removed from the filtrate under vacuum, giving **6** as a pale yellow powder (0.7610 g, 56% yield). The material was 98% pure by NMR spectroscopy. ^1H NMR (600 MHz, CD_2Cl_2): δ 7.77 (s, 8H, BArH), 7.62 (s, 4H, BArH), 6.56 (d, J = 8.6 Hz, 1H, ArH), 6.50 (d, J = 8.2 Hz, 1H, ArH), 4.50 (d, J = 15.2 Hz, 1H, crown-CH_2), 4.34 (m, 1H, crown-CH_2), 4.25 (m, 4H, Ar(CH_2)N, and crown-CH_2), 4.09 (m, 2H, crown-CH_2), 4.04 (m, 1H, crown-CH_2), 4.02 (m, 1H, crown-CH_2), 4.00 (t, J = 2.3 Hz 1H, crown-CH_2), 3.95 (dd, J = 4.1, 2.8 Hz 1H, crown-CH_2), 3.92 (m, 1H, crown-CH_2), 3.90 (t, J = 4.0 Hz, 1H, crown-CH_2), 3.83 (m, 1H, crown-CH_2), 3.81 (s, 3H, Ar(OCH_3)), 3.73 (m, 2H, crown-CH_2), 3.67 (t, J = 2.5 Hz, 1H, crown-CH_2), 3.64 (m, 2H, crown-CH_2), 3.57 (dt, J = 11.0, 4.1 Hz, 1H, crown-CH_2), 3.52 (m, 1H, crown-CH_2), 3.41 (dt, J = 13.5, 3.0 Hz, 1H, crown-CH_2), 3.13 (dq, J = 14.3, 2.8 Hz, 1H, crown-CH_2), 2.49 (n, J = 7.0 Hz, 1H, CH(CH_3)), 2.42 (p, J = 7.0 Hz, 1H, CH(CH_3)), 1.39 (dd, J = 14.9, 6.9 Hz, 3H, CH(CH_3)), 1.28 (dd, J = 15.3, 6.9 Hz, 3H, CH(CH_3)), 1.12 (dd, J = 20.3, 7.0 Hz, 3H, CH(CH_3)), 0.98 (dd, J = 16.4, 6.5 Hz, 3H, CH(CH_3)), and −29.86 (d, J = 27.4 Hz, 1H, IrH). $^{13}C\{^1H\}$ NMR (151 MHz, CD_2Cl_2): δ 162.12 (d, $^1J_{BC}$ = 49.9 Hz, B-C_{Ar}), 143.24 (d, J = 11.7 Hz, C_{Ar}), 137.34 (d, J = 4.3 Hz, C_{Ar}), 135.18 (C_{Ar}), 129.24 (q, $^2J_{FC}$ = 32.3 Hz, C_{BAr}-CF_3), 124.98 (q, $^1J_{FC}$ = 271.6 Hz, BAr-CF_3), 117.88 (sept, J = 3.8 Hz, C_{BAr}), 115.77 (C_{Ar}), 109.55 (C_{Ar}), 78.53 (crown-CH_2), 75.44 (crown-CH_2), 74.37 (crown-CH_2), 74.05 (crown-CH_2), 71.22 (crown-CH_2), 70.80 (crown-CH_2), 68.97 (Ar-(CH_2)N), 67.99 (crown-CH_2), 67.83 (crown-CH_2), 63.16 (Ar-(OCH_3)), 60.82 (crown-CH_2), 56.47 (crown-CH_2), 31.18 (d, $^1J_{PC}$ = 33.1 Hz, $CH(CH_3)_2$), 29.23 (d, $^1J_{PC}$ = 41.8 Hz, $CH(CH_3)_2$), 17.91 ($CH(CH_3)_2$), 16.82 (d, $^2J_{PC}$ = 8.2 Hz, $CH(CH_3)_2$), 16.68 ($CH(CH_3)_2$), and 16.56 ($CH(CH_3)_2$). $^{31}P\{^1H\}$ NMR (243 MHz, CD_2Cl_2): δ 142.42. HRMS: m/z calcd for ($\mathbf{6}^+$) 664.24, found m/z 664.23783. Anal. calcd for $C_{56}H_{54}BF_{24}IrNO_6P$: C, 44.05; H, 3.56; N, 0.92. Found: C, 43.20; H, 3.21; N, 0.86.

Procedure for Li^+ Dependence of Conversion to Arene Complex. In a glovebox, four 7.5 mM CD_2Cl_2 solutions of **1** were prepared in 20 mL scintillation vials, and increasing amounts of $LiBAr^F_4{\cdot}3Et_2O$ were added to each to create solutions that were 7.8, 16.9, 38.3, and 78.8 mM $LiBAr^F_4{\cdot}3Et_2O$. Allylbenzene (100 equiv) was added to each vial via syringe; then, the vials were sealed and allowed to stir for 16 h. After 16 h, the reaction mixtures were analyzed by NMR spectroscopy.

Procedure for Temperature Dependence of Conversion to Arene Complex. In a glovebox, a 20 mL vial was charged with 3.3 mg of **1**, 11.7 mg of $LiBAr^F_4{\cdot}3Et_2O$, and 441 μL of CD_2Cl_2, and the solution was transferred to a Teflon-sealed NMR tube. Allylbenzene (29.2 μL, 100 equiv) was added, and then the tube was sealed and heated at 35 °C for 16 h. The reaction was analyzed by NMR spectroscopy.

A separate 20 mL vial was charged with 4.4 mg of **1**, 15.4 mg of $LiBAr^F_4{\cdot}3Et_2O$, and 587 μL of 1,2-dichloroethane-d_4, and the solution was transferred to a Teflon-sealed NMR tube. Allylbenzene (38 μL, 100 equiv) was added; then, the tube was sealed and heated at 80 °C for 1 h. The reaction was analyzed by NMR spectroscopy.

Procedure for Allylbenzene Isomerization by [Li@(κ^2-^{15c5}NC′OP^{iPr})Ir(η^6-styrene)H][BAr^F_4]$_2$ (2). In a glovebox, a 20 mL scintillation vial was charged with 7.0 mg of **2**, 520 μL of CD_2Cl_2, and 3.6 μL of mesitylene internal standard. The solution was transferred to a Teflon-sealed NMR tube, 34 μL of allylbenzene was added, and the tube was sealed. Reaction progress was monitored via NMR spectroscopy.

Procedure for Arene Exchange Experiment Using Styrene-d_8. In a glovebox, a 20 mL scintillation vial was charged with 24.5 mg of **2** and 500 μL of CD_2Cl_2. The solution was transferred to a Teflon-sealed NMR tube, 10.4 μL styrene-d_8 (10 equiv) was added, and the tube was sealed. Reaction progress was monitored by NMR spectroscopy.

Procedure for Reaction of (6) with Styrene and $LiBAr^F_4{\cdot}3Et_2O$. In a glovebox, a 20 mL scintillation vial was charged with 10.4 of **6**, 11.3 mg of $LiBAr^F_4{\cdot}3Et_2O$, and 2 mL of CH_2Cl_2. Styrene (15.7 μL, 20 equiv) was added and the solution was allowed to stir for 30 min, at which time the solvent was removed under vacuum. The solids were washed with pentane and then dissolved in CD_2Cl_2 and analyzed by ^1H NMR spectroscopy.

Procedure for Reaction of (6) with Mesitylene and $LiBAr^F_4{\cdot}3Et_2O$. In a glovebox, a 20 mL scintillation vial was charged with 10.6 mg of **6**, 11.5 mg of $LiBAr^F_4{\cdot}3Et_2O$ (1.5 equiv), and 600 μL of CD_2Cl_2. Mesitylene (19.3 μL, 20 equiv) was added, and the solution was transferred to a Teflon-sealed NMR tube. The reaction was analyzed by ^1H and ^{31}P NMR spectroscopy after 30 min and 72 h, respectively.

Procedure for Reaction of (6) with Mesitylene and $LiAl(OC(CF_3)_3)_4$. In a glovebox, a 20 mL scintillation vial was charged with 11.8 mg of **6**, 12.3 mg of $LiAl(OC(CF_3)_3)_4$ (1.5 equiv), and 600 μL of CD_2Cl_2. Mesitylene (21.5 μL, 20 equiv) was added, and the mixture was transferred to a Teflon-sealed NMR tube. The reaction was analyzed by ^1H NMR spectroscopy after 30 min and 24 h, respectively.

Procedure for Catalyst Recycling Experiment. In a glovebox, two scintillation vials were each charged with iridium catalyst, $LiAl(OC(CF_3)_3)_4$, CD_2Cl_2, and mesitylene internal standard (in one vial: 4.9 mg of **1**, 7.2 mg of $LiAl(OC(CF_3)_3)_4$, 655 μL of CD_2Cl_2, 5 μL of mesitylene; in second vial: 4.8 mg of **5**, 7.0 mg of $LiAl(OC(CF_3)_3)_4$, 629 μL of CD_2Cl_2, 5 μL of mesitylene). Allylbenzene (100 equiv relative to iridium) was added to each vial via syringe. The vials were sealed and

https://dx.doi.org/10.1021/acscatal.0c03784
ACS Catal. 2020, 10, 13019−13030

allowed to stir for 20 min, and then the solutions were transferred to Teflon-sealed NMR tubes and ^{1}H NMR spectra were collected. The solutions were transferred back to scintillation vials, a second aliquot of allylbenzene was added (100 equiv), and the reactions were allowed to stir for 40 min. The solutions were then transferred to Teflon-sealed NMR tubes and ^{1}H NMR spectra were collected. The reactions were left in Teflon-sealed NMR tubes until both had reached completion, and then they were transferred back to scintillation vials and charged with a third aliquot of allylbenzene (100 equiv). After stirring for 80 min, the solutions were transferred to Teflon-sealed NMR tubes and ^{1}H NMR spectra were collected.

Procedure for Allylbenzene Comparison at Low Catalyst Loadings. In a glovebox, two 5 mM catalyst stock solutions were prepared in scintillation vials (catalyst **1**: 5.4 mg in 360 μL of 1,2-DCE-d_4; catalyst **6**: 5.2 mg in 340 μL of 1,2-DCE-d_4). Two one dram (4 mL) vials were then charged with 2.4 mg of $LiAl(OC(CF_3)_3)_4$ (5 equiv relative to iridium) each. To each one dram vial, 100 μL of catalyst stock solution and 400 μL of CD_2Cl_2 were added. The mixtures were transferred to Teflon-sealed NMR tubes and 33 μL of allylbenzene (500 equiv relative to iridium) was added to each. The tubes were sealed and heated at 70 °C for 9 h before ^{1}H NMR spectra were collected.

Procedure for 4-Phenyl-1-Butene Isomerization at Low Catalyst Loadings. In a glovebox, two 5 mM catalyst stock solutions were prepared in scintillation vials (catalyst **1**: 6.1 mg in 815 μL of CD_2Cl_2; catalyst **6**: 6.2 mg in 815 μL of CD_2Cl_2). Two one dram (4 mL) vials were then charged with 2.4 mg of $LiAl(OC(CF_3)_3)_4$ (5 equiv relative to iridium) each. To each one dram vial, 100 μL of catalyst stock solution, 400 μL of CD_2Cl_2, and 10 μL of mesitylene internal standard were added. The mixtures were transferred to Teflon-sealed NMR tubes and 37.5 μL of 4-phenyl-1-butene (500 equiv relative to iridium) was added to each. The tubes were sealed and heated at 40 °C for 5 h before ^{1}H NMR spectra were collected.

■ ASSOCIATED CONTENT

Supporting Information

The Supporting Information is available free of charge at https://pubs.acs.org/doi/10.1021/acscatal.0c03784.

NMR spectra and crystallographic details (PDF)

Crystallographic data (CIF)

Crystallographic data (CIF)

■ AUTHOR INFORMATION

Corresponding Author

Alexander J. M. Miller − *Department of Chemistry, University of North Carolina at Chapel Hill, Chapel Hill, North Carolina 27599-3290, United States;* orcid.org/0000-0001-9390-3951; Email: ajmm@email.unc.edu

Authors

Henry M. Dodge − *Department of Chemistry, University of North Carolina at Chapel Hill, Chapel Hill, North Carolina 27599-3290, United States*

Matthew R. Kita − *Department of Chemistry, University of North Carolina at Chapel Hill, Chapel Hill, North Carolina 27599-3290, United States*

Chun-Hsing Chen − *Department of Chemistry, University of North Carolina at Chapel Hill, Chapel Hill, North Carolina 27599-3290, United States;* orcid.org/0000-0003-0150-9557

Complete contact information is available at: https://pubs.acs.org/10.1021/acscatal.0c03784

Notes

The authors declare no competing financial interest.

■ ACKNOWLEDGMENTS

This material is based upon the work supported by the National Science Foundation under CAREER Award CHE-1553802. Mass spectrometry studies were supported by the National Science Foundation under Grant no. CHE-1726291.

■ REFERENCES

(1) Miller, A. J. M. Controlling Ligand Binding for Tunable and Switchable Catalysis: Cation-Modulated Hemilability in Pincer-Crown Ether Ligands. *Dalton Trans.* **2017**, *46*, 11987−12000.

(2) Blanco, V.; Leigh, D. A.; Marcos, V. Artificial Switchable Catalysts. *Chem. Soc. Rev.* **2015**, *44*, 5341−5370.

(3) Traut, T. *Allosteric Regulatory Enzymes*; Springer US: Boston, MA, 2008.

(4) Kovbasyuk, L.; Krämer, R. Allosteric Supramolecular Receptors and Catalysts. *Chem. Rev.* **2004**, *104*, 3161−3188.

(5) Wiester, M. J.; Ulmann, P. A.; Mirkin, C. A. Enzyme Mimics Based Upon Supramolecular Coordination Chemistry. *Angew. Chem., Int. Ed.* **2011**, *50*, 114−137.

(6) Kremer, C.; Lützen, A. Artificial Allosteric Receptors. *Chem. − Eur. J.* **2013**, *19*, 6162−6196.

(7) Ma, T.; Peng, Y.; Huang, W.; Ding, J. Molecular Mechanism of the Allosteric Regulation of the Aγ Heterodimer of Human NAD-Dependent Isocitrate Dehydrogenase. *Sci. Rep.* **2017**, *7*, No. 40921.

(8) Oliveri, C. G.; Ulmann, P. A.; Wiester, M. J.; Mirkin, C. A. Heteroligated Supramolecular Coordination Complexes Formed via the Halide-Induced Ligand Rearrangement Reaction. *Acc. Chem. Res.* **2008**, *41*, 1618−1629.

(9) Raynal, M.; Ballester, P.; Vidal-Ferran, A.; van Leeuwen, P. W. N. M. Supramolecular Catalysis. Part 1: Non-Covalent Interactions as a Tool for Building and Modifying Homogeneous Catalysts. *Chem. Soc. Rev.* **2014**, *43*, 1660−1733.

(10) Raynal, M.; Ballester, P.; Vidal-Ferran, A.; van Leeuwen, P. W. N. M. Supramolecular Catalysis. Part 2: Artificial Enzyme Mimics. *Chem. Soc. Rev.* **2014**, *43*, 1734−1787.

(11) McConnell, A. J.; Wood, C. S.; Neelakandan, P. P.; Nitschke, J. R. Stimuli-Responsive Metal−Ligand Assemblies. *Chem. Rev.* **2015**, *115*, 7729−7793.

(12) Vlatković, M.; Collins, B. S. L.; Feringa, B. L. Dynamic Responsive Systems for Catalytic Function. *Chem. − Eur. J.* **2016**, *22*, 17080−17111.

(13) Lifschitz, A. M.; Rosen, M. S.; McGuirk, C. M.; Mirkin, C. A. Allosteric Supramolecular Coordination Constructs. *J. Am. Chem. Soc.* **2015**, *137*, 7252−7261.

(14) Yoon, H. J.; Kuwabara, J.; Kim, J.-H.; Mirkin, C. A. Allosteric Supramolecular Triple-Layer Catalysts. *Science* **2010**, *330*, 66−69.

(15) Julliard, M.; Chanon, M. Photoelectron-Transfer Catalysis: Its Connections with Thermal and Electrochemical Analogs. *Chem. Rev.* **1983**, *83*, 425−506.

(16) Neilson, B. M.; Bielawski, C. W. Photoswitchable Metal-Mediated Catalysis: Remotely Tuned Alkene and Alkyne Hydroborations. *Organometallics* **2013**, *32*, 3121−3128.

(17) Broderick, E. M.; Guo, N.; Vogel, C. S.; Xu, C.; Sutter, J.; Miller, J. T.; Meyer, K.; Mehrkhodavandi, P.; Diaconescu, P. L. Redox Control of a Ring-Opening Polymerization Catalyst. *J. Am. Chem. Soc.* **2011**, *133*, 9278−9281.

(18) Allgeier, A. M.; Mirkin, C. A. Ligand Design for Electrochemically Controlling Stoichiometric and Catalytic Reactivity of Transition Metals. *Angew. Chem., Int. Ed.* **1998**, *37*, 894−908.

(19) Lorkovic, I. M.; Duff, R. R.; Wrighton, M. S. Use of the Redox-Active Ligand 1,1′-Bis(Diphenylphosphino)Cobaltocene To Reversibly Alter the Rate of the Rhodium(I)-Catalyzed Reduction and Isomerization of Ketones and Alkenes. *J. Am. Chem. Soc.* **1995**, *117*, 3617−3618.
(20) Gregson, C. K. A.; Gibson, V. C.; Long, N. J.; Marshall, E. L.; Oxford, P. J.; White, A. J. P. Redox Control within Single-Site Polymerization Catalysts. *J. Am. Chem. Soc.* **2006**, *128*, 7410−7411.
(21) Azoulay, J. D.; Koretz, Z. A.; Wu, G.; Bazan, G. C. Well-Defined Cationic Methallyl α-Keto-β-Diimine Complexes of Nickel. *Angew. Chem., Int. Ed.* **2010**, *49*, 7890−7894.
(22) Liberman-Martin, A. L.; Bergman, R. G.; Tilley, T. D. A Remote Lewis Acid Trigger Dramatically Accelerates Biaryl Reductive Elimination from a Platinum Complex. *J. Am. Chem. Soc.* **2013**, *135*, 9612−9615.
(23) Liberman-Martin, A. L.; Levine, D. S.; Liu, W.; Bergman, R. G.; Tilley, T. D. Biaryl Reductive Elimination Is Dramatically Accelerated by Remote Lewis Acid Binding to a 2,2′-Bipyrimidyl−Platinum Complex: Evidence for a Bidentate Ligand Dissociation Mechanism. *Organometallics* **2016**, *35*, 1064−1069.
(24) Bader, A.; Lindner, E. Coordination Chemistry and Catalysis with Hemilabile Oxygen-Phosphorus Ligands. *Coord. Chem. Rev.* **1991**, *108*, 27−110.
(25) Angell, S. E.; Rogers, C. W.; Zhang, Y.; Wolf, M. O.; Jones, W. E. Hemilabile Coordination Complexes for Sensing Applications. *Coord. Chem. Rev.* **2006**, *250*, 1829−1841.
(26) Braunstein, P.; Naud, F. Hemilability of Hybrid Ligands and the Coordination Chemistry of Oxazoline-Based Systems. *Angew. Chem., Int. Ed.* **2001**, *40*, 680−699.
(27) Yoo, C.; Dodge, H. M.; Miller, A. J. M. Cation-Controlled Catalysis with Crown Ether-Containing Transition Metal Complexes. *Chem. Commun.* **2019**, *55*, 5047−5059.
(28) Smith, J. B.; Kerr, S. H.; White, P. S.; Miller, A. J. M. Thermodynamic Studies of Cation−Macrocycle Interactions in Nickel Pincer-Crown Ether Complexes Enable Switchable Ligation. *Organometallics* **2017**, *36*, 3094−3103.
(29) Kita, M. R.; Miller, A. J. M. An Ion-Responsive Pincer-Crown Ether Catalyst System for Rapid and Switchable Olefin Isomerization. *Angew. Chem., Int. Ed.* **2017**, *56*, 5498−5502.
(30) Ivanova, S. M.; Nolan, B. G.; Kobayashi, Y.; Miller, S. M.; Anderson, O. P.; Strauss, S. H. Relative Lewis Basicities of Six $Al(OR^F)_4^-$ Superweak Anions and the Structures of LiAl{OCH-$(CF_3)_2$}$_4$ and [1-Et-3-Me-1,3-C3H3N2][Li{Al{OCH$(CF_3)_2$}$_4$}$_2$]. *Chem. − Eur. J.* **2001**, *7*, 503−510.
(31) Olgemöller, B.; Beck, W. A Cationic Ethylene(Hydrio)Iridium-(III) Complex. *Angew. Chem., Int. Ed.* **1980**, *19*, 834.
(32) Turlington, C. R.; Harrison, D. P.; White, P. S.; Brookhart, M.; Templeton, J. L. Probing the Oxidation Chemistry of Half-Sandwich Iridium Complexes with Oxygen Atom Transfer Reagents. *Inorg. Chem.* **2013**, *52*, 11351−11360.
(33) Jeong, H.; Joo, K. S.; Chin, C. S. Iridium(III) Complexes of H6-Arenes with Olefinic and Cyclopropyl Substituents: Facile Conversion to η^3-Phenylallyl Complexes. *Bull. Korean Chem. Soc.* **1997**, *18*, 402−405.
(34) Camp, A. M.; Kita, M. R.; Grajeda, J.; White, P. S.; Dickie, D. A.; Miller, A. J. M. Mapping the Binding Modes of Hemilabile Pincer-Crown Ether Ligands in Solution Using Diamagnetic Anisotropic Effects on NMR Chemical Shift. *Inorg. Chem.* **2017**, *56*, 11141−11150.
(35) Grajeda, J.; Kita, M. R.; Gregor, L. C.; White, P. S.; Miller, A. J. M. Diverse Cation-Promoted Reactivity of Iridium Carbonyl Pincer-Crown Ether Complexes. *Organometallics* **2016**, *35*, 306−316.
(36) Van der Zeijden, A. A. H.; Van Koten, G.; Luijk, R.; Grove, D. M. Formation of Octahedral Iridium(III) Dihydrides from the Reaction of Ortho-Chelated Aryliridium(I) Compounds with Dihydrogen. *Organometallics* **1988**, *7*, 1556−1561.
(37) Wingard, L. A.; Finniss, M. C.; Norris, M.; White, P. S.; Brookhart, M.; Templeton, J. L. Synthesis, Structure, and Reactivity of Iridium(III) Complexes Containing a 4,6-Dimethyl-1,3-Benzenediphenylimine Pincer Ligand. *Inorg. Chem.* **2013**, *52*, 515−526.
(38) Maitlis, P. M. (Pentamethylcyclopentadienyl)Rhodium and -Iridium Complexes: Approaches to New Types of Homogeneous Catalysts. *Acc. Chem. Res.* **1978**, *11*, 301−307.
(39) Goldman, A. S.; Landis, C. R.; Sen, A. Jack Halpern (1925-2018). *Angew. Chem., Int. Ed.* **2018**, *57*, 4460.
(40) Gregor, L. C.; Grajeda, J.; Kita, M. R.; White, P. S.; Vetter, A. J.; Miller, A. J. M. Modulating the Elementary Steps of Methanol Carbonylation by Bridging the Primary and Secondary Coordination Spheres. *Organometallics* **2016**, *35*, 3074−3086.
(41) Grotjahn, D. B.; Larsen, C. R.; Gustafson, J. L.; Nair, R.; Sharma, A. Extensive Isomerization of Alkenes Using a Bifunctional Catalyst: An Alkene Zipper. *J. Am. Chem. Soc.* **2007**, *129*, 9592−9593.
(42) Larsen, C. R.; Erdogan, G.; Grotjahn, D. B. General Catalyst Control of the Monoisomerization of 1-Alkenes to Trans -2-Alkenes. *J. Am. Chem. Soc.* **2014**, *136*, 1226−1229.
(43) Hassam, M.; Taher, A.; Arnott, G. E.; Green, I. R.; van Otterlo, W. A. L. Isomerization of Allylbenzenes. *Chem. Rev.* **2015**, *115*, 5462−5569.
(44) Larsen, C.; Paulson, E.; Erdogan, G.; Grotjahn, D. A Facile, Convenient, and Green Route to (E)-Propenylbenzene Flavors and Fragrances by Alkene Isomerization. *Synlett* **2015**, *26*, 2462−2466.
(45) Albéniz, A. C.; Espinet, P.; López-Fernández, R.; Sen, A. A Warning on the Use of Radical Traps as a Test for Radical Mechanisms: They React with Palladium Hydrido Complexes. *J. Am. Chem. Soc.* **2002**, *124*, 11278−11279.
(46) Biswas, S.; Huang, Z.; Choliy, Y.; Wang, D. Y.; Brookhart, M.; Krogh-Jespersen, K.; Goldman, A. S. Olefin Isomerization by Iridium Pincer Catalysts. Experimental Evidence for an η 3 -Allyl Pathway and an Unconventional Mechanism Predicted by DFT Calculations. *J. Am. Chem. Soc.* **2012**, *134*, 13276−13295.
(47) Chianese, A. R.; Shaner, S. E.; Tendler, J. A.; Pudalov, D. M.; Shopov, D. Y.; Kim, D.; Rogers, S. L.; Mo, A. Iridium Complexes of Bulky CCC-Pincer N-Heterocyclic Carbene Ligands: Steric Control of Coordination Number and Catalytic Alkene Isomerization. *Organometallics* **2012**, *31*, 7359−7367.
(48) Cooper, A. C.; Caulton, K. G. Identification of an Elusive Catalyst: IrH(η^2-$C_6H_4P^tBu_2$)(Cl)(P^tBu_2Ph) as a Precursor for C=C Bond Migration. *Inorg. Chim. Acta* **1996**, *251*, 41−51.
(49) Kita, M. R.; Miller, A. J. M. Cation-Modulated Reactivity of Iridium Hydride Pincer-Crown Ether Complexes. *J. Am. Chem. Soc.* **2014**, *136*, 14519−14529.
(50) Carreras, L.; Rovira, L.; Vaquero, M.; Mon, I.; Martin, E.; Benet-Buchholz, J.; Vidal-Ferran, A. Syntheses, Characterisation and Solid-State Study of Alkali and Ammonium BArF Salts. *RSC Adv.* **2017**, *7*, 32833−32841.
(51) Krossing, I.; Reisinger, A. Chemistry with Weakly-Coordinating Fluorinated Alkoxyaluminate Anions: Gas Phase Cations in Condensed Phases? *Coord. Chem. Rev.* **2006**, *250*, 2721−2744.
(52) Martínez-Martínez, A. J.; Weller, A. S. Solvent-Free Anhydrous Li^+, Na^+ and K^+ Salts of $[B(3,5\text{-}(CF_3)_2C_6H_3)_4]^-$, $[BAr_4^F]^-$. Improved Synthesis and Solid-State Structures. *Dalton Trans.* **2019**, *48*, 3551−3554.
(53) Yakelis, N. A.; Bergman, R. G. Safe Preparation and Purification of Sodium Tetrakis[(3,5-Trifluoromethyl)Phenyl]Borate ($NaBAr_{24}^F$): Reliable and Sensitive Analysis of Water in Solutions of Fluorinated Tetraarylborates. *Organometallics* **2005**, *24*, 3579−3581.

https://dx.doi.org/10.1021/acscatal.0c03784
ACS Catal. 2020, 10, 13019−13030